2015

Estimation of crop gross primary production (GPP): II. Do scaledMODIS vegetation indices improve performance?

Qingyuan Zhang
Universities Space Research Association, qyz72@yahoo.com

Yen-Ben Cheng
Sigma Space Corporation

Alexei I. Lyapustin
Climate and Radiation Laboratory

Yujie Wang
University of Maryland Baltimore County

Xiaoyang Zhang
South Dakota State University

See next page for additional authors

Authors
Qingyuan Zhang, Yen-Ben Cheng, Alexei I. Lyapustin, Yujie Wang, Xiaoyang Zhang, Andrew E. Suyker, Shashi Verma, Yanmin Shuai, and Elizabeth M. Middleton

Agricultural and Forest Meteorology 200 (2015) 1–8

Contents lists available at ScienceDirect

Agricultural and Forest Meteorology

journal homepage: www.elsevier.com/locate/agrformet

Estimation of crop gross primary production (GPP): II. Do scaled MODIS vegetation indices improve performance?

Qingyuan Zhang[a,b,*], Yen-Ben Cheng[c,b], Alexei I. Lyapustin[d], Yujie Wang[e,b], Xiaoyang Zhang[f], Andrew Suyker[g], Shashi Verma[g], Yanmin Shuai[h], Elizabeth M. Middleton[b]

[a] Universities Space Research Association, Columbia, MD 21044, USA
[b] Biospheric Sciences Laboratory, National Aeronautics and Space Administration/Goddard Space Flight Center, Greenbelt, MD 20771, USA
[c] Sigma Space Corporation, Lanham, MD 20706, USA
[d] Climate and Radiation Laboratory, Code 613, National Aeronautics and Space Administration Goddard Space Flight Center, Greenbelt, MD 20771, USA
[e] Goddard Earth Sciences and Technology Center, University of Maryland Baltimore County, Baltimore, MD 21228, USA
[f] Geospatial Sciences Center of Excellence, South Dakota State University, Brookings, SD 57007, USA
[g] School of Natural Resources, University of Nebraska–Lincoln, Lincoln, NE 68588, USA
[h] Earth Resources Technology, Inc., Laurel, MD 20707, USA

ARTICLE INFO

Article history:
Received 19 May 2014
Received in revised form 5 September 2014
Accepted 7 September 2014
Available online 28 September 2014

Keywords:
Daily GPP
MODIS
Vegetation index
$fAPAR_{chl}$

ABSTRACT

Satellite remote sensing estimates of gross primary production (GPP) have routinely been made using spectral vegetation indices (VIs) over the past two decades. The Normalized Difference Vegetation Index (NDVI), the Enhanced Vegetation Index (EVI), the green band Wide Dynamic Range Vegetation Index ($WDRVI_{green}$), and the green band Chlorophyll Index (CI_{green}) have been employed to estimate GPP under the assumption that GPP is proportional to the product of VI and photosynthetically active radiation (PAR) (where VI is one of four VIs: NDVI, EVI, $WDRVI_{green}$, or CI_{green}). However, the empirical regressions between VI*PAR and GPP measured locally at flux towers do not pass through the origin (i.e., the zero *X*–*Y* value for regressions). Therefore they are somewhat difficult to interpret and apply. This study investigates (1) what are the scaling factors and offsets (i.e., regression slopes and intercepts) between the fraction of PAR absorbed by chlorophyll of a canopy ($fAPAR_{chl}$) and the VIs and (2) whether the scaled VIs developed in (1) can eliminate the deficiency and improve the accuracy of GPP estimates. Three AmeriFlux maize and soybean fields were selected for this study, two of which are irrigated and one is rainfed. The four VIs and $fAPAR_{chl}$ of the fields were computed with the MODerate resolution Imaging Spectroradiometer (MODIS) satellite images. The GPP estimation performance for the scaled VIs was compared to results obtained with the original VIs and evaluated with standard statistics: the coefficient of determination (R^2), the root mean square error (RMSE), and the coefficient of variation (CV). Overall, the scaled EVI obtained the best performance. The performance of the scaled NDVI, EVI and $WDRVI_{green}$ was improved across sites, crop types and soil/background wetness conditions. The scaled CI_{green} did not improve results, compared to the original CI_{green}. The scaled green band indices ($WDRVI_{green}$, CI_{green}) did not exhibit superior performance to either the scaled EVI or NDVI in estimating crop daily GPP at these agricultural fields. The scaled VIs are more physiologically meaningful than original un-scaled VIs, but scaling factors and offsets may vary across crop types and surface conditions.

1. Introduction

Atmospheric general circulation models require quantification of land–atmosphere exchanges of energy, water and momentum, including CO_2 fluxes which can be provided by land surface process models (Bonan et al., 2011; Dickinson et al., 1993; Sellers et al., 1986). Satellite remote sensing offers inputs such as land cover types and the Normalized Difference Vegetation Index (NDVI) (Deering, 1978; Tucker, 1979) for use in the land surface modeling

* Corresponding author at: Building 33, Room G317, Biospheric Sciences Laboratory, Code 618, NASA/Goddard Space Flight Center, Greenbelt, MD 20771, USA. Tel.: +1 3016146672; fax: +1 301 614 6695.
E-mail address: qyz72@yahoo.com (Q. Zhang).

http://dx.doi.org/10.1016/j.agrformet.2014.09.003
0168-1923/© 2014 Elsevier B.V. All rights reserved.

(Dickinson et al., 1990; Sellers et al., 1994). Pioneering work (Asrar et al., 1992; Myneni et al., 1997; Running et al., 2000; Sellers, 1987) has shown the fraction of photosynthetically active radiation (PAR) absorbed by a canopy/vegetation (FPAR, i.e., $fAPAR_{canopy}$) can be approximated with NDVI (Running et al., 2000). Therefore, NDVI has been employed to estimate vegetation gross primary productivity (GPP) in a variation (as GPP = ε*NDVI*PAR, Running et al., 2000), inspired by the logic from the light use efficiency (LUE) model (Monteith, 1972, 1977):

$$GPP = \varepsilon * fAPAR_{PSN} * PAR = \varepsilon * APAR_{PSN}, \quad (1)$$

where ε is LUE for vegetation photosynthesis (PSN) (Running et al., 2000) and $fAPAR_{PSN}$ is the fraction of PAR absorbed for PSN ($APAR_{PSN}$). Monitoring changes in crop GPP with satellite remote sensing data advances the capability to understand and manage global food security, sustainability practices, and environmental impacts, and to study global carbon cycle and global water cycle.

The three-band Enhanced Vegetation Index (EVI) (Huete et al., 1997) and the two-band EVI (called EVI2, Jiang et al., 2008) have also been utilized to predict terrestrial GPP in a similar way as GPP = ε*EVI*PAR (Jin et al., 2013; Kalfas et al., 2011; King et al., 2011; Li et al., 2007; Mahadevan et al., 2008; Schubert et al., 2012; Sjöström et al., 2011; Wu et al., 2008, 2010, 2011, 2012; Xiao et al., 2004; Yan et al., 2009). In addition, Gitelson and colleagues also explored the application of the green band Wide Dynamic Range Vegetation Index ($WDRVI_{green}$) and the green band Chlorophyll Index (CI_{green}) for crop GPP estimation, in addition to the NDVI and EVI (Gitelson et al., 2008, 2012; Peng and Gitelson, 2011, 2012; Peng et al., 2011).

However, since the empirical regressions between the VI*PAR products and GPP measured locally at flux towers do not pass through the origin (i.e., the zero *X*–*Y* value for regressions) and produce offsets, they are somewhat difficult to interpret and apply (Gitelson et al., 2012; Sims et al., 2006; Zhang et al., 2014b). This is considered to be a source of error affecting the accuracy and reliability of remote sensing GPP estimates based on VIs. In the literature, there is no paper that presents how to scale the VIs in space and time to solve the problem.

The standard MODerate resolution Imaging Spectroradiometer (MODIS) 8-day GPP product (MOD17A2 GPP) uses the MOD15A2 FPAR (a $fAPAR_{canopy}$) product as a model input (Running et al., 2004; Zhao and Running, 2008). Investigations to find the scaling factor and offset of NDVI through $fAPAR_{canopy}$–NDVI functions have been conducted, where $fAPAR_{canopy} = a_0$*NDVI + b_0 (a_0 is the scaling factor or slope, and b_0 is *y*-intercept or offset) (Fensholt et al., 2004; Goward and Huemmrich, 1992; Knyazikhin et al., 1998, 2002; Potter et al., 1993; Prince and Goward, 1995; Randerson et al., 1996; Sellers et al., 1996; Sims et al., 2005). However, the MOD15A2 FPAR product overestimates in situ $fAPAR_{canopy}$ during spring greenup and fall senescent periods, and underestimates in situ $fAPAR_{canopy}$ in mid-summer during peak GPP activity at the agricultural fields we selected [see (Zhang et al., 2014a) for details].

We developed an algorithm to retrieve the fraction of PAR absorbed by chlorophyll throughout the canopy ($fAPAR_{chl}$) from actual MODIS observations or from synthesized 30 m MODIS-spectral-like observations simulated with EO-1 Hyperion images (Zhang, 2003; Zhang et al., 2005, 2009, 2012, 2013, 2014c). We found that $fAPAR_{chl} \neq fAPAR_{canopy}$, and that the fraction of PAR absorbed by foliage non-chlorophyll components ($fAPAR_{non-chl}$) varies with types and seasonally (Zhang et al., 2013). Zhang et al. (2014a) presented the performance of $fAPAR_{chl}$ and MOD15A2 FPAR in crop GPP estimation, and concluded that $fAPAR_{chl}$ is superior to MOD15A2 FPAR. Zhang et al. (2014b) investigated the performance of original un-scaled VIs in GPP estimation, and suggested that further investigation on the performance of scaled VIs should be carried out.

The objectives of this paper are straightforward: (1) to explore how surface conditions affect the scaling factors ("*a*") and offsets ("*b*") derived through regression analysis of $fAPAR_{chl}$ vs. the four VIs: $fAPAR_{chl} = a$*VI + b for each crop type (corn, soybean) per field; (2) to investigate how much the scaled VIs can improve the prediction accuracy of GPP estimates compared to the prediction of original un-scaled VIs.

2. Methods

2.1. Study sites and tower data

The three AmeriFlux crop sites for corn, or maize (*Zea mays* L.) and soybean (*Glycine max* [L.] Merr.) used in this study are located at the University of Nebraska–Lincoln (UNL) Agricultural Research and Development Center near Mead, Nebraska (US-NE1, US-NE2 and US-NE3). The first two fields are circular (radius ∼390 m) and equipped with center-pivot irrigation systems (US-NE1, 41°09′54.2″ N, 96°28′35.9″ W; US-NE2, 41°09′53.6″ N, 96°28′07.5″ W). The third is a 790 m long square field (US-NE3, 41°10′46.7″ N, 96°26′22.4″ W) that relies entirely on rainfall. Each field is equipped with an eddy covariance flux tower (Gitelson et al., 2006, 2012; Peng et al., 2013). The first field (US-NE1) is a continuous maize field while the other two fields are maize–soybean rotation fields (soybean is planted in even years).

Tower eddy-covariance carbon exchange, PAR, and GPP measurements in growing season from 2001 to 2006 are publically available and can be downloaded from ftp://cdiac.ornl.gov/pub/ameriflux/data. The nighttime ecosystem respiration/temperature Q_{10} relationship was used to estimate the daytime ecosystem respiration (Baldocchi, 2003). Daily GPP was computed by subtracting respiration (*R*) from net ecosystem exchange (NEE), i.e., GPP = NEE − *R* (Suyker et al., 2005). These sites provided the opportunity to examine the semi-empirical relationships between $fAPAR_{chl}$ versus VIs for both C4 (maize) and C3 (soybean) crops in both irrigated and non-irrigated ecosystems, and to investigate the benefits of employing the scaled relationships to estimate GPP.

2.2. Remote sensing data processing and GPP estimation

Six years (2001–2006) of MODIS L1B calibrated radiance data (MOD021KM and MOD02HKM) and geolocation data (MOD03) covering the three study sites were downloaded from https://ladsweb.nascom.nasa.gov:9400/data/. Two of the MODIS bands have a nadir spatial resolution of 250 m: B1 (red, 620–670 nm) and B2 (near infrared, NIR_1, 841–876 nm). The MODIS land bands 3–7 have a nadir spatial resolution of 500 m: B3 (blue, 459–479 nm), B4 (green, 545–565 nm), B5 (NIR_2, 1230–1250 nm), B6 (shortwave infrared, $SWIR_1$, 1628–1652 nm) and B7 ($SWIR_2$, 2105–2155 nm). The centers of the original 500 m grids defined in the standard surface reflectance product (MOD09) that encompass the three tower sites are not the centers of the three fields and vegetation in each of the original 500 m grids is not homogeneous (see Fig. 2 of Guindin-Garcia et al., 2012). The MODIS gridding procedure for the standard MOD09 product does not ensure the gridded surface reflectance covers the entire grid (Wolfe et al., 1998). A modified gridding procedure was used for this study (Zhang et al., 2014b), whereby the centers of the three 500 m grids were matched to the centers of the three fields, respectively. The L1B radiance data from each swath were gridded at 500 m resolution for MODIS bands 1–7 with area weight of each MODIS observation. This modified gridding processing was incorporated into the Multi-Angle Implementation of Atmospheric Correction (MAIAC) algorithm (Lyapustin et al., 2008, 2011a,b, 2012). MAIAC is an advanced algorithm which uses time series analysis and a combination of pixel-based and image-based processing to improve cloud/snow detection, and to achieve more accurate aerosol retrievals and atmospheric correction, based on the bidirectional reflectance distribution function (BRDF) model of the surface.

Derived bidirectional reflectance factors (BRF, also called directional surface reflectance) in MODIS bands 1–7 were used for this study. The impact of MODIS observation footprint size resulting from variable view zenith angle (VZA) on crop daily GPP estimation for these sites was recently reported elsewhere (Zhang et al., 2014b). In order to eliminate the potential bias due to large VZAs, only observations with VZA $\leq 35^{\circ}$ were included in this study. The surface reflectance data (ρ) were used to calculate the following indices (Deering, 1978; Gitelson, 2004; Gitelson et al., 2007, 2012; Huete et al., 1997, 2002; Tucker, 1979):

$$\mathrm{CI_{green}} = \frac{\rho \mathrm{NIR_1}}{\rho_{\mathrm{green}}} - 1 \quad (2)$$

$$\mathrm{WDRVI_{green}} = \frac{0.3\rho\mathrm{NIR_1} - \rho_{\mathrm{green}}}{0.3\rho_{\mathrm{NIR_1}} + \rho_{\mathrm{green}}} + \frac{1-0.3}{1+0.3} \quad (3)$$

$$\mathrm{NDVI} = \frac{\rho\mathrm{NIR_1} - \rho_{\mathrm{red}}}{\rho\mathrm{NIR_1} + \rho_{\mathrm{red}}} \quad (4)$$

$$\mathrm{EVI} = 2.5\frac{\rho_{\mathrm{NIR_1}} - \rho_{\mathrm{red}}}{1 + \rho_{\mathrm{NIR_1}} + 6\rho_{\mathrm{red}} - 7.5\rho_{\mathrm{blue}}} \quad (5)$$

We used the PROSAIL2 model (Jacquemoud and Baret, 1990; Baret and Fourty, 1997; Braswell et al., 1996; Verhoef, 1984, 1985; Zhang et al., 2005, 2009, 2012, 2013), a coupled soil-canopy-leaf radiative transfer model, to retrieve $\mathrm{fAPAR_{chl}}$, the fraction of PAR absorbed by the foliage of the canopy ($\mathrm{fAPAR_{foliage}}$), and the fraction of PAR absorbed by the non-photosynthetic foliage components ($\mathrm{fAPAR_{non\text{-}chl}}$) (Zhang et al., 2014a). A pixel is composed of canopy and soil (Zhang et al., 2009, 2012, 2013). The canopy is partitioned into foliage and stem (including branch), and the foliage component is further partitioned into chlorophyll (chl) and non-chlorophyll (non-chl) components, where non-chl is composed of non-photosynthetic pigments (referred to as brown pigment) and dry matter (Baret and Fourty, 1997). The surface reflectances of MODIS bands 1–7 are used for retrieval of fAPAR variables (Zhang et al., 2009, 2012, 2013, 2014c):

$$\mathrm{fAPAR_{non\text{-}chl}} = \mathrm{fAPAR_{brown\_pigment}} + \mathrm{fAPAR_{dry\_matter}} \quad (6)$$

$$\mathrm{fAPAR_{foliage}} = \mathrm{fAPAR_{chl}} + \mathrm{fAPAR_{non\text{-}chl}} \quad (7)$$

$$\mathrm{fAPAR_{canopy}} = \mathrm{fAPAR_{foliage}} + \mathrm{fAPAR_{stem}} \quad (8)$$

The scaling factors ("*a*") and offsets ("*b*") of VIs were derived from linear regression through $\mathrm{fAPAR_{chl}}$–VI functions for each crop type per field, where $\mathrm{fAPAR_{chl}} = a^*\mathrm{VI} + b$ (VIs = NDVI, EVI, $\mathrm{WDRVI_{green}}$, and $\mathrm{CI_{green}}$).

The product of VIs and tower daily PAR (VI*PAR) and the product of scaled VIs and daily PAR (scaled VI*PAR) were compared against the tower daily GPP for each crop type per field (GPP = $\bar{\varepsilon}_0 * \mathrm{VI} * \mathrm{PAR}$ or GPP = $\bar{\varepsilon} * \text{scaled VI} * \mathrm{PAR}$). The coefficients '$\bar{\varepsilon}_0$' and '$\bar{\varepsilon}$' were computed with a least squares best fit algorithm. The computed values for $\bar{\varepsilon}_0$ and $\bar{\varepsilon}$ were then used to predict GPP, and coefficient of determination (R^2), the root mean square error (RMSE, $\mathrm{g\,C\,m^{-2}\,d^{-1}}$) and coefficient of variation (CV, %) was calculated. The average light use efficiency at chlorophyll level ($\mathrm{LUE_{chl}}$, i.e., $\bar{\varepsilon}_{\mathrm{chl}}$) was computed using GPP = $\mathrm{LUE_{chl}}^*\mathrm{fAPAR_{chl}}^*$PAR with a least squares best fit algorithm. Improvements of crop daily GPP estimation using scaled VIs were assessed.

3. Results

The scaling factor ("*a*", also called slope) and offset ("*b*", also called *y*-intercept) obtained through the regression functions $\mathrm{fAPAR_{chl}} = a^*\mathrm{VI} + b$ for each crop per field are listed in Table 1, where the statistics for the R^2, RMSE and *x*-intercept are also summarized. The *x*-intercepts of $\mathrm{fAPAR_{chl}} = a^*\mathrm{VI} + b$ give minimum VI values at zero $\mathrm{fAPAR_{chl}}$. The 95% confidence intervals of slope, *y*-intercept and *x*-intercept for each crop per field are reported, too. The $\mathrm{CI_{green}}$ is a simple ratio index while the other three VIs include consideration of normalization. The confidence intervals for $\mathrm{CI_{green}}$ are different from those for other three VIs for each type per field. For each crop type in irrigated fields USNE1 and USNE2, the confidence intervals of *y*-intercepts and *x*-intercepts for NDVI, EVI and $\mathrm{CI_{green}}$ are different from each other. For each crop type in rainfed field USNE3, the confidence intervals of *y*-intercepts and *x*-intercepts for NDVI and $\mathrm{CI_{green}}$ overlap each other, but are different from those for EVI. Mean values of the confidence intervals of the slopes, *y*-intercepts and *x*-intercepts vary with VIs, sites, crop types and irrigation options. None of the *y*-intercepts or *x*-intercepts for NDVI, EVI or $\mathrm{WDRVI_{green}}$ is close to the origin (i.e., zero *X*–*Y* point).

The functions in Table 1 were used to compute the scaled values of NDVI, EVI, $\mathrm{WDRVI_{green}}$ and $\mathrm{CI_{green}}$ for each crop type per field. For instance, for the NDVI at US-NE1: scaled NDVI = 1.11*NDVI – 0.29. The coefficients $\bar{\varepsilon}_0$ and $\bar{\varepsilon}$ and $\mathrm{LUE_{chl}}$ of each crop per field are listed in Table 2. Corn $\mathrm{LUE_{chl}}$ is ~1.6 times of soybean $\mathrm{LUE_{chl}}$ (Table 2), which agrees with the expectation that C4 plants have higher LUE than C3 plants (e.g., Prince, 1991), and explains why maize displays a wider daily GPP range (~34 $\mathrm{g\,C\,m^{-2}\,d^{-1}}$) than soybean (~19 $\mathrm{g\,C\,m^{-2}\,d^{-1}}$) (Zhang et al., 2014b). The coefficients $\bar{\varepsilon}_0$ and $\bar{\varepsilon}$ were applied to estimate crop daily GPP.

Fig. 1 shows the estimated soybean daily GPP for the rainfed field US-NE3 using the four original VIs with $\bar{\varepsilon}_0$ and the scaled VIs with $\bar{\varepsilon}$, compared to tower daily GPP. The scaled NDVI, EVI and $\mathrm{WDRVI_{green}}$ combined with $\bar{\varepsilon}$ had better GPP estimation performance than the original counterparts, respectively, demonstrating higher R^2 and lower RMSE. Compared to the original counterparts, the (scaled NDVI)*PAR, the (scaled EVI)*PAR and the (scaled $\mathrm{WDRVI_{green}}$)*PAR values were closer to 0 when GPP = 0. The scaled $\mathrm{CI_{green}}$ did not provide better GPP estimation than the original $\mathrm{CI_{green}}$. In order to save pages, similar figures for US-NE1, US-NE2 and figures for maize in US-NE3 are not presented in this paper.

Table 3 summarized the statistics (R^2, RMSE and CV) for estimating crop daily GPP using the original VIs with $\bar{\varepsilon}_0$ and the scaled VIs with $\bar{\varepsilon}$, respectively. These statistics show that the best performance was obtained with the scaled EVI while the least successful performance among the four scaled VIs was obtained with $\mathrm{CI_{green}}$ across the sites, crop types and irrigation/rainfed options. For example at the US-NE1 site, scaled EVI and scaled $\mathrm{CI_{green}}$ had contrasting best/worst performances in GPP estimation: R^2: 0.88/0.77, RMSE: 2.92/4.05 $\mathrm{g\,C\,m^{-2}\,d^{-1}}$, and CV: 19%/26% (Table 3). GPP estimates for corn had better performance than for soybean using scaled NDVI and EVI for sites US-NE2 and US-NE3. Better results might be achieved for the sites examined in other studies (King et al., 2011; Sjöström et al., 2009) if the scaled EVI (through coefficients obtained from the regression of $\mathrm{fAPAR_{chl}}$ vs. EVI) had been utilized.

For each crop in any field, the scaled NDVI, EVI and $\mathrm{WDRVI_{green}}$ improved the prediction performance of crop daily GPP while the scaled $\mathrm{CI_{green}}$ did not, compared to the original un-scaled VIs. GPP improvements for the three that benefited from scaling, ranked from most to least were the NDVI, $\mathrm{WDRVI_{green}}$, EVI, for which the R^2 increased (↑: 0.16, 0.13, 0.09), RMSE decreased (↓: 0.95, 0.78, 0.65 $\mathrm{g\,C\,m^{-2}\,d^{-1}}$), and the CV also decreased (↓: 8%, 6%, 5%). The improvements also varied with crop types and irrigation conditions. For example, the NDVI improvement for soybean (R^2, ↑ 0.20; CV, ↓9%) was better than for corn (R^2, ↑0.13; CV, ↓7%), and the average improvement for the rainfed field (R^2, ↑0.21; RMSE, ↓1.10 $\mathrm{g\,C\,m^{-2}\,d^{-1}}$; and CV, ↓10%) was better than for the irrigation fields (R^2, ↑0.12; RMSE, ↓0.85 $\mathrm{g\,C\,m^{-2}\,d^{-1}}$; and CV, ↓6%).

Table 1
List of relationships between $fAPAR_{chl}$ and VIs for the three crop sites ($y = ax + b$, y: $fAPAR_{chl}$, x: VI). The 95% confidence intervals of slope ("a"), y-intercept ("b"), and x-intercept are presented. Coefficients of determination (R^2) and root mean square error (RMSE) are also presented.

		NDVI	EVI	$WDRVI_{green}$	CI_{green}
US-NE1 (maize, irrigated)	Function	$y = 1.11x - 0.29$	$y = 1.30x - 0.18$	$y = 1.13x - 0.39$	$y = 0.13x - 0.13$
	Slope 95% confidence interval	(1.07, 1.14)	(1.26, 1.34)	(1.09, 1.17)	(0.12, 0.13)
	y-Intercept 95% confidence interval	(−0.31, −0.27)	(−0.20, −0.17)	(−0.41, −0.37)	(−0.14, −0.11)
	x-Intercept 95% confidence interval	(0.26, 0.27)	(0.14, 0.15)	(0.34, 0.35)	(0.92, 1.04)
	R^2	0.95	0.96	0.94	0.94
	RMSE	0.06	0.05	0.06	0.06
US-NE2 (maize, irrigated)	Function	$y = 1.10x - 0.27$	$y = 1.29x - 0.16$	$y = 1.11x - 0.37$	$y = 0.12x - 0.10$
	Slope 95% confidence interval	(1.07, 1.14)	(1.25, 1.34)	(1.07, 1.15)	(0.11, 0.12)
	y-Intercept 95% confidence interval	(−0.29,−0.25)	(−0.18, −0.15)	(−0.40, −0.35)	(−0.12, −0.08)
	x-Intercept 95% confidence interval	(0.24, 0.25)	(0.12, 0.13)	(0.33, 0.34)	(0.72, 0.91)
	R^2	0.96	0.96	0.95	0.93
	RMSE	0.05	0.05	0.06	0.08
US-NE2 (soybean, irrigated)	Function	$y = 1.06x - 0.25$	$y = 1.21x - 0.16$	$y = 1.04x - 0.32$	$y = 0.11x - 0.08$
	Slope 95% confidence interval	(1.03, 1.10)	(1.18, 1.24)	(1.00, 1.08)	(0.10, 0.12)
	y-Intercept 95% confidence interval	(−0.27, −0.23)	(−0.17, −0.14)	(−0.34, −0.30)	(−0.10, −0.06)
	x-Intercept 95% confidence interval	(0.23, 0.24)	(0.12, 0.13)	(0.30, 0.31)	(0.58, 0.81)
	R^2	0.95	0.97	0.94	0.89
	RMSE	0.05	0.05	0.06	0.08
US-NE3 (maize, rainfed)	Function	$y = 1.25x–0.43$	$y = 1.46x - 0.25$	$y = 1.13x - 0.39$	$y = 0.11x - 0.02$
	Slope 95% confidence interval	(1.12, 1.38)	(1.34, 1.59)	(1.00, 1.26)	(0.10, 0.13)
	y-Intercept 95% confidence interval	(−0.51, −0.34)	(−0.30, −0.19)	(−0.48, −0.30)	(−0.08, 0.04)
	x-Intercept 95% confidence interval	(0.33, 0.35)	(0.16, 0.18)	(0.33, 0.36)	(0.05, 0.37)
	R^2	0.82	0.87	0.78	0.73
	RMSE	0.07	0.06	0.07	0.08
US-NE3 (soybean, rainfed)	Function	$y = 1.29x - 0.44$	$y = 1.37x - 0.24$	$y = 1.07x - 0.35$	$y = 0.10x + 0.03$
	Slope 95% confidence interval	(1.18, 1.40)	(1.28, 1.46)	(0.95, 1.19)	(0.08,0.11)
	y-Intercept 95% confidence interval	(−0.52, −0.37)	(−0.29, −0.19)	(−0.44, −0.26)	(−0.04,0.09)
	x-Intercept 95% confidence interval	(0.33,0.36)	(0.17,0.18)	(0.31, 0.35)	(−0.57, −0.02)
	R^2	0.91	0.94	0.85	0.77
	RMSE	0.06	0.05	0.08	0.10

Table 2
List of the coefficient $\bar{\varepsilon}_0$ in $GPP = \bar{\varepsilon}_0 * VI * PAR$, the coefficient $\bar{\varepsilon}$ in $GPP = \bar{\varepsilon} * \text{scaled VI} * PAR$, and LUE_{chl} in $GPP = LUE_{chl} * fAPAR_{chl} * PAR$ (unit: $g\,C\,mol^{-1}$ PPFD).

	LUE_{chl}	NDVI		EVI		$WDRVI_{green}$		CI_{green}	
		$\bar{\varepsilon}_0$	$\bar{\varepsilon}$	$\bar{\varepsilon}_0$	$\bar{\varepsilon}$	$\bar{\varepsilon}_0$	$\bar{\varepsilon}$	$\bar{\varepsilon}_0$	$\bar{\varepsilon}$
UE-NE1 (corn, irrigated)	0.65	0.48	0.68	0.65	0.67	0.44	0.68	0.07	0.66
US-NE2 (corn, irrigated)	0.65	0.49	0.66	0.66	0.65	0.45	0.66	0.07	0.65
US-NE2 (soybean, irrigated)	0.42	0.31	0.43	0.40	0.42	0.28	0.43	0.04	0.45
US-NE3 (corn, rainfed)	0.71	0.45	0.73	0.67	0.72	0.43	0.73	0.08	0.72
US-NE3 (soybean, rainfed)	0.43	0.28	0.44	0.39	0.44	0.26	0.44	0.04	0.44

Table 3
Coefficients of determination (R^2), root mean square errors (RMSE, $g\,C\,m^{-2}\,d^{-1}$) and coefficients of variation (CV) for simulated GPP with the VIs using two options: original unscaled VIs versus scaled VIs, compared to tower daily GPP.

		NDVI		EVI		$WDRVI_{green}$		CI_{green}	
		Original	Scaled	Original	Scaled	Original	Scaled	Original	Scaled
US-NE1 (corn)	R^2	0.67	0.80	0.80	0.88	0.67	0.80	0.77	0.77
	RMSE	4.85	3.77	3.74	2.92	4.88	3.84	4.05	4.05
	CV	31%	24%	24%	19%	32%	25%	26%	26%
US-NE2 (corn)	R^2	0.72	0.81	0.83	0.88	0.71	0.77	0.72	0.72
	RMSE	4.38	3.62	3.40	2.83	4.42	3.95	4.39	4.37
	CV	26%	22%	21%	17%	27%	24%	26%	26%
US-NE2 (soybean)	R^2	0.63	0.78	0.75	0.84	0.65	0.79	0.73	0.73
	RMSE	3.16	2.45	2.61	2.11	3.09	2.43	2.76	2.75
	CV	31%	24%	26%	21%	30%	24%	27%	27%
US-NE3 (corn)	R^2	0.63	0.80	0.70	0.81	0.62	0.76	0.68	0.69
	RMSE	4.66	3.44	4.14	3.32	4.68	3.75	4.32	4.31
	CV	33%	25%	30%	24%	34%	27%	31%	31%
US-NE3 (soybean)	R^2	0.50	0.75	0.63	0.76	0.52	0.72	0.66	0.66
	RMSE	3.35	2.38	2.88	2.35	3.29	2.51	2.79	2.79
	CV	36%	26%	31%	26%	36%	27%	30%	30%

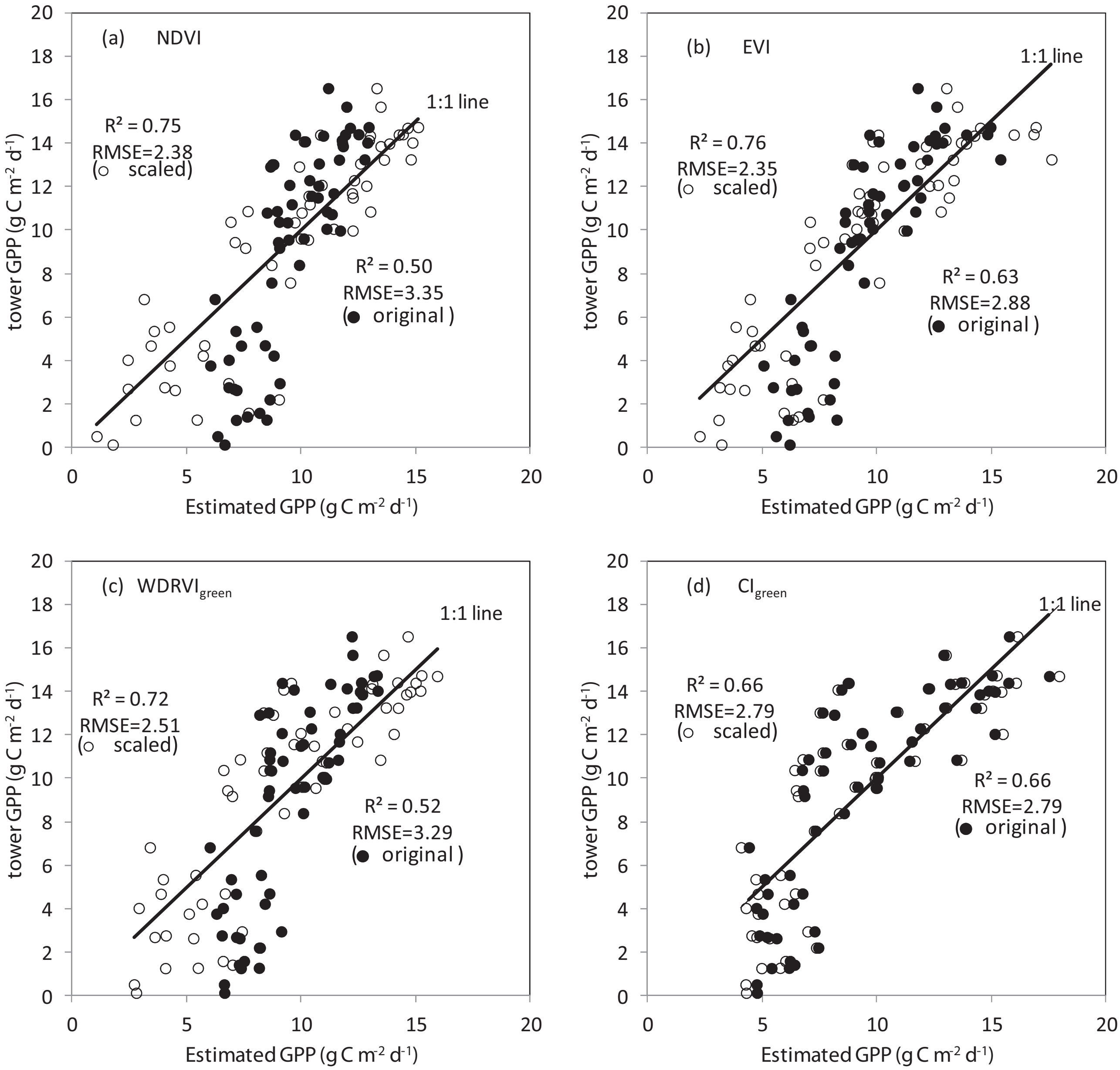

Fig. 1. Comparison between tower daily GPP vs. estimated daily GPP for the US-NE3 site (soybean): (a) NDVI; (b) EVI; (c) $WDRVI_{green}$; and (d) CI_{green}. Filled circles use original un-scaled VIs while empty circles use scaled VIs. Only observations with $VZA \leq 35^{\circ}$ are included.

4. Discussion

The PSROAIL2 model well distinguishes vegetation from soil and $fAPAR_{chl}$ retrieved with the PROSAIL2 model excludes the impact of soil/background (Zhang et al., 2012, 2013). The $fAPAR_{foliage}$ comprises chlorophyll and non-chlorophyll foliage fractions ($fAPAR_{chl}$, $fAPAR_{non\text{-}chl}$). Therefore, the PAR absorbed by non-photosynthetic vegetation components (NPV) of the canopy is excluded from $APAR_{chl}$ since $APAR_{chl} = fAPAR_{chl}$*PAR. This is the theoretical basis for potential improvement of GPP estimation using the scaled VIs. The *x*-intercept values of the semi-empirical linear functions of $fAPAR_{chl}$ vs. VI in Table 1 have an important biophysical meaning: there is not any chlorophyll showing up at the pixel when its un-scaled VI is less than its *x*-intercept value. Gitelson and Colleagues (2007) reported that, before green-up when green leaves do not appear, MODIS 250 m NDVI values for the fields could be greater than 0.2, which is close to the minimum *x*-intercepts of NDVI (0.23, Table 1) we found with MODIS 500 m images. In irrigated fields, the mean values of the *x*-intercept confidence intervals for EVI were about half of those for NDVI, and about 1/3 as large as those for $WDRVI_{green}$ (Table 1). In rainfed fields, the mean values of the *x*-intercept confidence intervals for EVI were about half of those for both NDVI and $WDRVI_{green}$ (Table 1). Soil/background wetness has less impact on EVI than on NDVI which is consistent with the original idea that inspired the development of EVI (Huete, 1988; Huete et al., 1997). Daughtry et al. (2000) has expressed that VIs combined with NIR and red bands are less impacted by background than VIs combined with NIR and green bands. Earlier studies (Sims et al., 2006, 2008) have shown that GPP drops to zero at variable EVI values (i.e., *x*-intercept EVI values) in their selected flux sites, and have found the minimum *x*-intercept value is ~0.1. So Sims et al. (2008) has developed a GPP model using EVI – 0.1 instead of the original EVI. The *x*-intercept confidence intervals of EVI in the three fields (US-NE1, US-NE2 and US-NE3) ranged from (0.12, 0.13), (0.14, 0.15) to (0.16, 0.18). Our findings are consistent with earlier empirical studies (Daughtry et al., 2000; Huete, 1988; Huete et al., 1997; Sims et al., 2006, 2008). Furthermore, the scaled VIs with scaling factors and offsets using the semi-empirical relationships between $fAPAR_{chl}$ vs. VIs for each crop type per field are more physiologically meaningful (Table 1) than the original un-scaled VIs.

The $\bar{\varepsilon}$ estimates for all scaled VIs are close to the relevant LUE_{chl} values for each crop type per field. In contrast, the $\bar{\varepsilon}_0$ estimates associated with the original un-scaled NDVI and $WDRVI_{green}$ are lower than the relevant LUE_{chl} values. The $\bar{\varepsilon}_0$ estimates for CI_{green} are much lower than the relevant LUE_{chl} values because the original un-scaled CI_{green} range (~1 to 10) is much wider than the scaled CI_{green} range (~0 to ~1). It is worth noting that both the $\bar{\varepsilon}_0$ and the $\bar{\varepsilon}$ estimates for the original EVI and the scaled EVI are close to the physiologically relevant LUE_{chl} values. This partly explains the reasonableness and success of the Vegetation Photosynthesis Model (VPM) (Xiao et al., 2004) which assumes GPP = ε*EVI*PAR. This study suggests that the GPP estimation made with the VPM may be improved by replacing the original EVI with $fAPAR_{chl}$, or by scaling the EVI using the relationship between $fAPAR_{chl}$ and EVI.

The R^2 between tower daily GPP and estimated GPP with scaled VIs for all cases ranges from 0.66 to 0.88 while the RMSE (CV) between them ranges from 4.37 to 2.11 $g\,C\,m^{-2}\,d^{-1}$ (from 31% to 17%). Although the R^2 between $fAPAR_{chl}$ and scaled VI is high for all cases (0.73–0.97), the RMSE between $fAPAR_{chl}$ and scaled VI varies with crop type, irrigation/rainfed options, and VI options, which caused the variation of the performance of estimated GPP with scaled VIs. Among the four scaled VIs, the RMSE between $fAPAR_{chl}$ and the scaled EVI is smallest and the R^2 is highest for all study sites. For US-NE2 and US-NE3, the RMSE between $fAPAR_{chl}$ and scaled CI_{green} is biggest and the R^2 is lowest.

5. Conclusion

This study exhibited improvement in the performance of crop daily GPP estimation using scaled NDVI, EVI and $WDRVI_{green}$, compared to their original un-scaled counterparts. However, performance improvement of crop daily GPP estimation using scaled CI_{green} was not observed. The irrigated fields have better performance, as compared to the rainfed field. The performance also varied with crop types and VI options. The scaled EVI provided the best performance among all cases. This study does not find that the scaled $WDRVI_{green}$ or the scaled CI_{green} is superior to the scaled NDVI or scaled EVI in predicting crop daily GPP.

Compared to the original VIs, the scaled VIs developed with the semi-empirical relationships between $fAPAR_{chl}$ and VIs are more physiologically meaningful. However, the scaling factors and offsets (and x-intercepts) vary field by field, and vary type by type. Investigations to explore the scaling factors and offsets of these VIs using $fAPAR_{chl}$ for other plant functional types should be carried out in the future. We will explore how the scaling factors and offsets change over space and time, and vary with climate. Investigations on whether scaled EVI is best for all fields and all types among the four scaled VIs are also needed. We suggest an approach whereby MODIS-derived VIs are scaled pixel by pixel. This approach provides scaled VIs for use when $fAPAR_{chl}$ is unavailable. We expect that future research on GPP simulation based on the biochemical or land surface modeling (Bounoua et al., 2000; Potter et al., 2003; Sellers et al., 1994, 1996) will achieve reduced uncertainty and improved accuracy when the scaled MODIS VIs replace the original VIs.

Acknowledgments

This study was supported by NASA Terrestrial Ecology Project (Grant No. NNX12AJ51G; PI, Q. Zhang) and NASA Science of Terra and Aqua Project (Grant No. NNX14AK50G; PI, Q. Zhang) (Dr. Diane Wickland, Manager). We would like to thank the support and the use of facilities and equipment provided by the Center for Advanced Land Management Information Technologies and the Carbon Sequestration program, University of Nebraska–Lincoln. Site-specific climate and CO_2 flux data are distributed by AmeriFlux network (http://public.ornl.gov/ameriflux), supported by Carbon Dioxide Information Analysis Center at the Oak Ridge National Laboratory of the Department of Energy. We are grateful to anonymous reviewers whose comments helped improve the paper.

References

Asrar, G., Myneni, R.B., Choudhury, B.J., 1992. Spatial heterogeneity in vegetation canopies and remote-sensing of absorbed photosynthetically active radiation – a modeling study. Remote Sens. Environ. 41, 85–103.

Baldocchi, D.D., 2003. Assessing the eddy covariance technique for evaluating carbon dioxide exchange rates of ecosystems: past, present and future. Global Change Biol. 9, 479–492.

Bonan, G.B., Lawrence, P.J., Oleson, K.W., Levis, S., Jung, M., Reichstein, M., Lawrence, D.M., Swenson, S.C., 2011. Improving canopy processes in the Community Land Model version 4 (CLM4) using global flux fields empirically inferred from FLUXNET data. J. Geophys. Res. 116, G02014.

Baret, F., Fourty, T., 1997. Radiometric estimates of nitrogen status in leaves and canopies. In: Lemaire, G. (Ed.), Diagnosis of the Nitrogen Status in Crops. Springer, Berlin, pp. 201–227.

Bounoua, L., Collatz, G.J., Los, S.O., Sellers, P.J., Dazlich, D.A., Tucker, C.J., Randal, D.A., 2000. Sensitivity of climate to changes in NDVI. J. Clim. 13, 2277–2292.

Braswell, B.H., Schimel, D.S., Privette, J.L., Moore, B., Emery, W.J., Sulzman, E.W., et al., 1996. Extracting ecological and biophysical information from AVHRR optical data: an integrated algorithm based on inverse modeling. J. Geophys. Res. Atmos. 101, 23335–23348.

Daughtry, C.S.T., Walthall, C.L., Kim, M.S., de Colstoun, E.B., McMurtrey, J.E., 2000. Estimating corn leaf chlorophyll concentration from leaf and canopy reflectance. Remote Sens. Environ. 74, 229–239.

Deering, D.W., 1978. Rangeland Reflectance Characteristics Measured by Aircraft and Spacecraft Sensors. Texas A&M University, College Station, TX, pp. 338.

Dickinson, R.E., Henderson-Sellers, A., Kennedy, P.J., 1993. Biosphere-Atmosphere Transfer Scheme (BATS) Version 1e as Coupled to the NCAR Community Climate Model. Tech. Note NCAR/TN-387+STR. Natl. Center for Atmos. Res., Boulder, CO.

Dickinson, R.E., Pinty, B., Verstraete, M.M., 1990. Relating surface albedos in GCM to remotely sensed data. Agric. For. Meteorol. 52, 109–131.

Fensholt, R., Sandholt, I., Rasmussen, M.S., 2004. Evaluation of MODIS LAI, fAPAR and the relation between fAPAR and NDVI in a semi-arid environment using in situ measurements. Remote Sens. Environ. 91, 490–507.

Gitelson, A.A., 2004. Wide dynamic range vegetation index for remote quantification of biophysical characteristics of vegetation. J. Plant Physiol. 161, 165–173.

Gitelson, A.A., Peng, Y., Masek, J.G., Rundquist, D.C., Verma, S., Suyker, A., Baker, J.M., Hatfield, J.L., Meyers, T., 2012. Remote estimation of crop gross primary production with Landsat data. Remote Sens. Environ. 121, 404–414.

Gitelson, A.A., Viña, A., J.G. M., Verma, S.B., Suyker, A.E., 2008. Synoptic monitoring of gross primary productivity of maize using Landsat data. IEEE Geosci. Remote Sens. Lett. 5, 133–137.

Gitelson, A.A., Viña, A., Verma, S.B., Rundquist, D.C., Arkebauer, T.J., Keydan, G., Leavitt, B., Ciganda, V., Burba, G.G., Suyker, A.E., 2006. Relationship between gross primary production and chlorophyll content in crops: implications for the synoptic monitoring of vegetation productivity. J. Geophys. Res. 111, D08S11.

Gitelson, A.A., Wardlow, B.D., Keydan, G.P., Leavitt, B., 2007. An evaluation of MODIS 250-m data for green LAI estimation in crops. Geophys. Res. Lett. 34, L20403.

Goward, S.N., Huemmrich, K.F., 1992. Vegetation canopy PAR absorptance and the normalized difference vegetation index – an assessment using the SAIL model. Remote Sens. Environ. 39, 119–140.

Guindin-Garcia, N., Gitelson, A.A., Arkebauer, T.J., Shanahan, J., Weiss, A., 2012. An evaluation of MODIS 8- and 16-day composite products for monitoring maize green leaf area index. Agric. For. Meteorol. 161, 15–25.

Huete, A., Didan, K., Miura, T., Rodriguez, E.P., Gao, X., Ferreira, L.G., 2002. Overview of the radiometric and biophysical performance of the MODIS vegetation indices. Remote Sens. Environ. 83, 195–213.

Huete, A.R., 1988. A soil-adjusted vegetation index (SAVI). Remote Sens. Environ. 25, 295–309.

Huete, A.R., Liu, H.Q., Batchily, K., vanLeeuwen, W., 1997. A comparison of vegetation indices global set of TM images for EOS-MODIS. Remote Sens. Environ. 59, 440–451.

Jacquemoud, S., Baret, F., 1990. PROSPECT—a model of leaf optical properties spectra. Remote Sens. Environ. 34, 75–91.

Jiang, Z., Huete, A.R., Didan, K., Miura, T., 2008. Development of a two-band Enhanced Vegetation Index without a blue band. Remote Sens. Environ. 112, 3833–3845.

Jin, C., Xiao, X.M., Merbold, L., Arneth, A., Veenendaal, E., Kutsch, W., 2013. Phenology and gross primary production of two dominant savanna woodland ecosystems in Southern Africa. Remote Sens. Environ. 135, 189–201.

Kalfas, J., Xiao, X., Vanegas, D., Verma, S., Suyker, A.E., 2011. Modeling gross primary production of irrigated and rain-fed maize using MODIS imagery and CO(2) flux tower data. Agric. For. Meteorol. 151, 1514–1528.

King, D.A., Turner, D.P., Ritts, W.D., 2011. Parameterization of a diagnostic carbon cycle model for continental scale application. Remote Sens. Environ. 115, 1653–1664.

Knyazikhin, Y., Martonchik, J.V., Myneni, R.B., Diner, D.J., Running, S.W., 1998. Synergistic algorithm for estimating vegetation canopy leaf area index and fraction of absorbed photosynthetically active radiation from MODIS and MISR data. J. Geophys. Res. 103, 32257–32275.

Knyazikhin, Y., Zhao, M., Nemani, R., Privette, J.L., Shabanov, N., Myneni, R.B., Running, S.W., 2002. MODIS LAI/FPAR Team Response to BigFoot Validation Results. http://cybele.bu.edu/modismisr/validation/response.pdf

Li, Z., Yu, G., Xiao, X., Li, Y., Zhao, X., Ren, C., Zhang, L., Fu, Y., 2007. Modeling gross primary production of alpine ecosystems in the Tibetan Plateau using MODIS images and climate data. Remote Sens. Environ. 107, 510–519.

Lyapustin, A., Martonchik, J., Wang, Y., Laszlo, I., Korkin, S., 2011a. Multi-angle implementation of atmospheric correction (MAIAC): Part 1. Radiative transfer basis and look-up tables. J. Geophys. Res. 116, D03210.

Lyapustin, A., Wang, Y., Frey, R., 2008. An automatic cloud mask algorithm based on time series of MODIS measurements. J. Geophys. Res., 113.

Lyapustin, A., Wang, Y., Laszlo, I., Hilker, T., Hall, F., Sellers, P., Tucker, J., Korkin, S., 2012. Multi-angle implementation of atmospheric correction for MODIS (MAIAC). 3: Atmospheric correction. Remote Sens. Environ. 127, 385–393.

Lyapustin, A., Wang, Y., Laszlo, I., Kahn, R., Korkin, S., Remer, L., Levy, R., Reid, J.S., 2011b. Multi-angle implementation of atmospheric correction (MAIAC): Part 2. Aerosol algorithm. J. Geophys. Res. 116, D03211.

Mahadevan, P., Wofsy, S.C., Matross, D.M., Xiao, X., Dunn, A.L., Lin, J.C., Gerbig, C., Munger, J.W., Chow, V.Y., Gottlieb, E.W., 2008. A satellite-based biosphere parameterization for net ecosystem CO_2 exchange: vegetation photosynthesis and respiration model (VPRM). Global Biogeochem. Cycles 22, GB2005 (2001–2017).

Monteith, J.L., 1972. Solar-radiation and productivity in tropical ecosystems. J. Appl. Ecol. 9, 747–766.

Monteith, J.L., 1977. Climate and efficiency of crop production in Britain. Phil. Trans. R. Soc. Lond. B: Biol. Sci. 281, 277–294.

Myneni, R.B., Nemani, R.R., Running, S.W., 1997. Estimation of global leaf area index and absorbed PAR using radiative transfer models. IEEE Trans. Geosci. Remote Sens. 35, 1380–1393.

Peng, Y., Gitelson, A.A., 2011. Application of chlorophyll-related vegetation indices for remote estimation of maize productivity. Agric. For. Meteorol. 151, 1267–1276.

Peng, Y., Gitelson, A.A., 2012. Remote estimation of gross primary productivity in soybean and maize based on total crop chlorophyll content. Remote Sens. Environ. 117, 440–448.

Peng, Y., Gitelson, A.A., Keydan, G.P., Rundquist, D.C., Moses, W.J., 2011. Remote estimation of gross primary production in maize and support for a new paradigm based on total crop chlorophyll content. Remote Sens. Environ. 115, 978–989.

Peng, Y., Gitelson, A.A., Sakamoto, T., 2013. Remote estimation of gross primary productivity in crops using MODIS 250 m data. Remote Sens. Environ. 128, 186–196.

Potter, C., Klooster, S., Myneni, R., Genovese, V., Tan, P.N., Kumar, V., 2003. Continental-scale comparisons of terrestrial carbon sinks estimated from satellite data and ecosystem modeling 1982–1998. Global Planet. Change 39, 201–213.

Potter, C.S., Randerson, J.T., Field, C.B., Matson, P.A., Vitousek, P.M., Mooney, H.A., Klooster, S.A., 1993. Terrestrial ecosystem production – a process model-based on global satellite and surface data. Global Biogeochem. Cycles 7, 811–841.

Prince, S.D., 1991. A model of regional primary production for use with coarse resolution satellite data. Int. J. Remote Sens. 12, 1313–1330.

Prince, S.D., Goward, S.N., 1995. Global primary production: a remote sensing approach. J. Biogeogr. 22, 815–835.

Randerson, J.T., Thompson, M.V., Malmstrom, C.M., Field, C.B., Fung, I.Y., 1996. Substrate limitations for heterotrophs: implications for models that estimate the seasonal cycle of atmospheric CO_2. Global Biogeochem. Cycles 10, 585–602.

Running, S., Nemani, R., Heinsch, F., Zhao, M., Reeves, M., Hashimoto, H., 2004. A continuous satellite-derived measure of global terrestrial primary production. Bioscience 54, 547–560.

Running, S.W., Thornton, P.E., Nemani, R., Glassy, J.M., 2000. Global terrestrial gross and net primary productivity from the earth observing system. In: Sala, O.E., Jackson, R.B., Mooney, H.A., Howarth, R.W. (Eds.), Methods in Ecosystem Science. Springer-Verlag, New York, pp. 44–57.

Schubert, P., Lagergren, F., Aurela, M., Christensen, T., Grelle, A., Heliasz, M., Klemedtsson, L., Lindroth, A., Pilegaard, K., Vesala, T., Eklundh, L., 2012. Modeling GPP in the Nordic forest landscape with MODIS time series data—comparison with the MODIS GPP product. Remote Sens. Environ. 126, 136–147.

Sellers, P., 1987. Canopy reflectance, photosynthesis, and transpiration: II. The role of biophysics in the linearity of their interdependence. Remote Sens. Environ. 21, 143–183.

Sellers, P.J., Los, S.O., Tucker, C.J., Justice, C.O., Dazlich, D.A., Collatz, G.J., Randall, D.A., 1996. A revised land surface parameterization (SiB2) for atmospheric GCMs. II: The generation of global fields of terrestrial biophysical parameters from satellite data. J. Clim. 9, 706–737.

Sellers, P.J., Mintz, Y., Sud, Y.C., Dalcher, A., 1986. A simple biosphere model (SIB) for use within general circulation models. J. Atmos. Sci. 43, 505–531.

Sellers, P.J., Tucker, C.J., Collatz, G.J., Los, S.O., Justice, C.O., Dazlich, D.A., Randall, D.A., 1994. A global 1° by 1° NDVI data set for climate studies: Part 2. The generation of global fields of terrestrial biophysical parameters from the NDVI. Int. J. Remote Sens. 15, 3519–3545.

Sims, D.A., Rahman, A.F., Cordova, V.D., Baldocchi, D.D., Flanagan, L.B., Goldstein, A.H., Hollinger, D.Y., Misson, L., Monson, R.K., Schmid, H.P., Wofsy, S.C., Xu, L.K., 2005. Midday values of gross CO_2 flux and light use efficiency during satellite overpasses can be used to directly estimate eight-day mean flux. Agric. For. Meteorol. 131, 1–12.

Sims, D.A., Rahman, A.F., Cordova, V.D., El-Masri, B.Z., Baldocchi, D.D., Bolstad, P.V., Flanagan, L.B., Goldstein, A.H., Hollinger, D.Y., Misson, L., Monson, R.K., Oechel, W.C., Schmid, H.P., Wofsy, S.C., Xu, L., 2008. A new model of gross primary productivity for North American ecosystems based solely on the Enhanced Vegetation Index and land surface temperature from MODIS. Remote Sens. Environ. 112, 1633–1646.

Sims, D.A., Rahman, A.F., Cordova, V.D., El-Masri, B.Z., Baldocchi, D.D., Flanagan, L.B., Goldstein, A.H., Hollinger, D.Y., Misson, L., Monson, R.K., Oechel, W.C., Schmid, H.P., Wofsy, S.C., Xu, L., 2006. On the use of MODIS EVI to assess gross primary productivity of North American ecosystems. J. Geophys. Res. 111, 1–16.

Sjöström, M., Ardö, J., Eklundh, L., El-Tahir, B.A., El-Khidir, H.A.M., Hellström, M., Pilesjö, P., Seaquist, J., 2009. Evaluation of satellite based indices for gross primary production estimates in a sparse savanna in the Sudan. Biogeosciences 6, 129–138.

Sjöström, M., Ardö, J., Arneth, A., Boulain, N., Cappelaere, B., Eklundh, L., Grandcourt, A.D., Kutsch, W.L., Merbold, L., Nouvellon, Y., Scholes, R.J., Schubert, P., Seaquist, J., Veenendaal, E.M., 2011. Exploring the potential of MODIS EVI for modeling gross primary production across African ecosystems. Remote Sens. Environ. 115, 1081–1089.

Suyker, A.E., Verma, S.B., Burba, G.G., Arkebauer, T.J., 2005. Gross primary production and ecosystem respiration of irrigated maize and irrigated soybean during a growing season. Agric. For. Meteorol. 131, 180–190.

Tucker, C.J., 1979. Red and photographic infrared linear combinations for monitoring vegetation. Remote Sens. Environ. 8, 127–150.

Verhoef, W., 1984. Light-scattering by leaf layers with application to canopy reflectance modeling—the SAIL model. Remote Sens. Environ. 16, 125–141.

Verhoef, W., 1985. Earth observation modeling based on layer scattering matrices. Remote Sens. Environ. 17, 165–178.

Wolfe, R., Roy, D., Vermote, E., 1998. The MODIS land data storage, gridding and compositing methodology: level 2 grid. IEEE Trans. Geosci. Remote Sens. 36, 1324–1338.

Wu, C., Chen, J.M., Desai, A.R., Hollinger, D.Y., Arain, M.A., Margolis, H.A., Gough, C.M., Staebler, R.M., 2012. Remote sensing of canopy light use efficiency in temperate and boreal forests of North America using MODIS imagery. Remote Sens. Environ. 118, 60–72.

Wu, C., Chen, J.M., Huang, N., 2011. Predicting gross primary production from the Enhanced Vegetation Index and photosynthetically active radiation: evaluation and calibration. Remote Sens. Environ. 115, 3424–3435.

Wu, C., Niu, Z., Gao, S., 2010. Gross primary production estimation from MODIS data with vegetation index and photosynthetically active radiation in maize. J. Geophys. Res. 115, 1–12.

Wu, W., Wang, S., Xiao, X., Yu, G., Fu, Y., Hao, Y., 2008. Modeling gross primary production of a temperate grassland ecosystem in Inner Mongolia, China, using MODIS imagery and climate data. Sci. China Ser. D: Earth Sci. 51, 1–12.

Xiao, X.M., Hollinger, D., Aber, J., Goltz, M., Davidson, E.A., Zhang, Q., Moore, B., 2004. Satellite-based modeling of gross primary production in an evergreen needleleaf forest. Remote Sens. Environ. 89, 519–534.

Yan, H., Fu, Y., Xiao, X., Huang, H.Q., He, H., Ediger, L., 2009. Modeling gross primary productivity for winter wheat–maize double cropping system using MODIS time series and CO_2 eddy flux tower data. Agric. Ecosyst. Environ. 129, 391–400.

Zhang, Q., 2003. Improving estimation of terrestrial gross primary productivity (GPP): retrieval of fraction of photosynthetically active radiation absorbed by chlorophyll (fAPARchl) versus FAPAR. In: NASA Earth System Science (ESS) Fellowship Program.

Zhang, Q., Cheng, Y.-B., Lyapustin, A.I., Wang, Y., Gao, F., Suyker, A., Verma, S., Middleton, E.M., 2014a. Estimation of crop gross primary production (GPP): MOD15A2 FPAR versus fAPARchl. Remote Sens. Environ. 153, 1–6.

Zhang, Q., Cheng, Y.-B., Lyapustin, A.I., Wang, Y., Xiao, X., Suyker, A., Verma, S., Tan, B., Middleton, E.M., 2014b. Estimation of crop daily gross primary production (GPP): I. Impact of MODIS observation footprint area and impact of vegetation BRDF characteristics. Agric. For. Meteorol. 191, 51–63.

Zhang, Q., Middleton, E.M., Cheng, Y.-B., Landis, D.R., 2013. Variations of foliage chlorophyll fAPAR and foliage non-chlorophyll fAPAR ($fAPAR_{chl}$, $fAPAR_{non\text{-}chl}$) at the Harvard forest. IEEE J. Sel. Top. Appl. Earth Obs. Remote Sens. 6, 2254–2264.

Zhang, Q., Middleton, E.M., Cheng, Y.-B., Huemmrich, K.F., Cook, B.D., Corp, L.A., Kustas, W.P., Russ, A.L., Prueger, J.H., 2014c. Remote estimation of corn daily gross primary production (GPP): integration of $fAPAR_{chl}$ and PRI. Agric. For. Meteorol. (under review).

Zhang, Q., Middleton, E.M., Gao, B.-C., Cheng, Y.-B., 2012. Using EO-1 Hyperion to simulate HyspIRI products for a coniferous forest: the fraction of PAR absorbed by chlorophyll ($fAPAR_{chl}$) and leaf water content (LWC). IEEE Trans. Geosci. Remote Sens. 50, 1844–1852.

Zhang, Q., Middleton, E.M., Margolis, H.A., Drolet, G.G., Barr, A.A., Black, T.A., 2009. Can a MODIS-derived estimate of the fraction of PAR absorbed by chlorophyll ($FAPAR_{chl}$) improve predictions of light-use efficiency and ecosystem photosynthesis for a boreal aspen forest? Remote Sens. Environ. 113, 880–888.

Zhang, Q., Xiao, X.M., Braswell, B., Linder, E., Baret, F., Moore, B., 2005. Estimating light absorption by chlorophyll, leaf and canopy in a deciduous broadleaf forest using MODIS data and a radiative transfer model. Remote Sens. Environ. 99, 357–371.

Zhao, M., Running, S.W., 2008. Remote sensing of terrestrial primary production and carbon cycle. In: Liang, S. (Ed.), Advances in Land Remote Sensing. Springer Science Business Media, New York, pp. 423–444, ISBN: 978-1-4020-6449-4.